Common and Distinct Roles of DFos and DJun During *Drosophila* Development

Juan R. Riesgo-Escovar and Ernst Hafen*

The *Drosophila* homolog of c-Jun regulates epithelial cell shape changes during the process of dorsal closure in mid-embryogenesis. Here, mutations in the *DFos* gene are described. In dorsal closure, DFos cooperates with DJun by regulating the expression of *dpp*; Dpp acts as a relay signal that triggers cell shape changes and *DFos* expression in neighboring cells. In addition to the joint requirement of DFos and DJun during dorsal closure, DFos functions independently of DJun during early stages of embryogenesis. These findings demonstrate common and distinct roles of DFos and DJun during embryogenesis and suggest a conserved link between AP-1 (activating protein-1) and TGF-β (transforming growth factor–β) signaling during epithelial cell shape changes.

The AP-1 transcription factor complex is activated in response to various stimuli, including cytokines, growth factors, and cellular stresses like ultraviolet irradiation or heat shock. Active AP-1 complexes are dimers of basic-region leucine zipper (bZip) transcription factors, formed predominantly by members of the Jun and Fos gene families (*1*). In vertebrates, the number of related Jun and Fos family members has complicated analysis of AP-1 function in vivo. c-*fos* mutant mice are viable and possess defects in bone formation, whereas c-*jun* mutant mice die at mid-gestation with liver defects (*2*). In *Drosophila*, single homologs of c-Jun and c-Fos, DJun and DFra (here referred to as DFos), have been identified (*3*, *4*). Like c-Jun, DJun forms homodimers and heterodimers with DFos and binds to AP-1 DNA binding sites. In contrast to mammalian c-Fos, however, DFos also forms homodimers, suggesting DJun-independent functions (*3*). DJun mutant embryos die as a result of failed dorsal closure (*5*–*7*). Dorsal closure occurs during mid-embryogenesis and results in stretching of the lateral epithelia over the extraembryonic membrane and fusion at the dorsal mid-line. In addition to DJun, mutations in genes encoding Jun NH_2-terminal kinase kinase (DJNKK), *hep*, and Jun NH_2-terminal kinase (DJNK), *bsk*, also block this cell shape change, and thus, dorsal closure (*8*–*10*). Expression of *dpp* in the most dorsal row of cells, the leading edge, is dependent on DJun, DJNK, and DJNKK function (*5*, *6*, *11*). Mutations in genes encoding the Dpp receptors Tkv and Put result in a similar phenotype (*12*). Expression of activated Tkv receptors in the embryonic ectoderm partially rescues the dorsal closure defect of DJNK mutants. We proposed that activation of the DJNK pathway by an unknown signal results in stretching of the leading edge cells and that Dpp acts as a relay signal to induce stretching of more ventrally located ectodermal cells (*8*).

We identified a genetic locus, *kayak* (*kay*), that has an embryonic lethal phenotype similar to *DJun* mutants (*13*). The kay^1 allele contains a restriction-site polymorphism in the DFos coding region caused by a single point mutation resulting in an in-frame stop codon at position 1045 of the DFos sequence (Fig. 1, A and B). Expression of the *DFos* cDNA in the ectoderm completely rescued the dorsal closure defect of homozygous kay^1 and kay^1/kay^2 mutants (Fig. 1D) (*14*). Thus, DFos is encoded by *kay*, and loss of DFos function results in a phenotype similar to that of DJun mutants. A fraction of rescued kay^1/kay^2 mutants survived to become adults with split thoraxes (Fig. 1E). The dorsal thorax is made during metamorphosis from the proximal portions of the left and right wing imaginal discs by fusion of these primordia on the dorsal side. The split-thorax phenotype is reminiscent of phenotypes described for rare homozygous *hep* mutant flies (*9*). This similarity suggested that DJNKK and DFos are not only required for

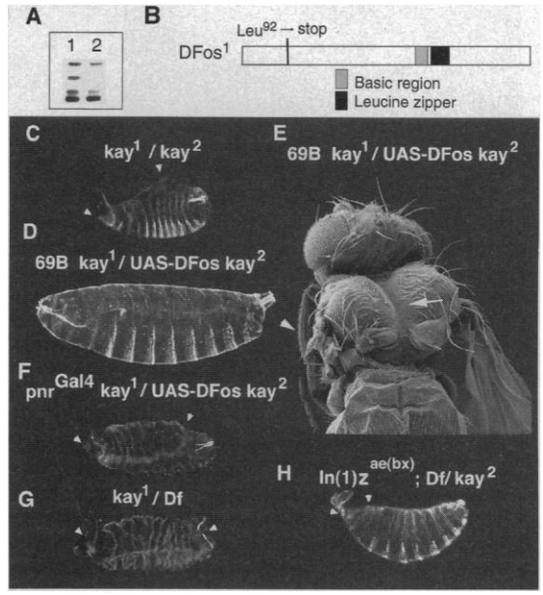

Fig. 1. DFos is encoded by the *kay* locus. (**A**) Southern blot analysis of $kay^1/TM3$ balancer (lane 1) and control (lane 2) genomic DNA digested with Hinc II. The probe used was the DFos cDNA. (**B**) Depiction of the mutation in kay^1 resulting in the change of a Leu to a stop codon within a Hinc II site at position 1045 of the published sequence (*3*). The mutation is a T to A transition in the following sequence: CCC ACG TT(A)G ACG (mutant in parentheses). Polymerase chain reaction amplification of mutant and control DNA and sequencing were done as in (*5*). Control DNA was from the kay^2 mutation, because it was induced in the same background and recovered in the same mutagenesis. In the regions sequenced, the kay^2 sequences coded for the same amino acids as the published *DFos* sequence (*3*). (**C**) Embryonic cuticular phenotype of a kay^1/kay^2 trans-heterozygote. The dorsal cuticle is partially missing (white arrowheads), and the embryo is open dorsally. In this and subsequent figures, dorsal is up and anterior is to the left unless otherwise noted; in all cuticle preparations, white arrowheads mark the extent of the dorsal hole in the cuticle. All embryos are shown at the same magnification. Cuticle preparations were done as in (*8*). (**D**) The embryonic phenotype of *kay* mutants is rescued by ectodermal expression of *DFos*. Mutant transheterozygous *kay* embryos are completely closed dorsally when *DFos* is expressed in the ectoderm under the control of the 69B Gal4 line. (**E**) Expression of *DFos* can partially rescue *kay* mutants to pharate adults. Dorsal aspect of a rescued *kay* mutant heteroallelic combination. All rescued adults had a split thorax (arrow), indicating a failure of the dorsal portion of the imaginal epithelia to fuse properly, and frequently lacked one wing because of improper eversion of the wing blade (large arrowhead). (**F**) DFos is required in lateral ectodermal cells ventral to the leading edge cells during closure. Transheterozygous mutant *kay* embryos where *DFos* was expressed in the leading edge cells and three to four rows of lateral ectodermal cells ventral to the leading edge cells by means of the $pannier^{MD237}$ Gal4 line (*17*) were not rescued. (**G**) kay^1 behaves genetically as a null allele: The $kay^1/Df\ (3R)01215$ embryo is completely open dorsally [compare with the partially closed embryo in (C) and the kay^1 homozygote in Fig. 2A]. (**H**) The *kay* locus shows transvection: $kay^2/Df\ (3R)01215$ fails to complement only in a $In(1)z^{ae(bx)}$ homozygous mutant background, known to inhibit transvection. The noncomplementing embryos show mild dorsal-open phenotypes. All mutants and *Drosophila* stocks not described in (*5*) are described in (*16*).

Zoologisches Institut, Universität Zürich, Winterthurerstrasse 190, CH-8057 Zürich, Switzerland.

*To whom correspondence should be addressed. E-mail: hafen@zool.unizh.ch

dorsal closure of embryonic epithelia but also for the dorsal joining of imaginal epithelia during pupal development.

The similarity of the DJun and DFos mutant phenotypes and the genetic interactions between *DFos*, *DJun*, and *DJNK* mutants suggested that these factors cooperate in vivo. Like *DJun* mutations, *DFos* null alleles completely blocked shape changes that normally occur in the leading edge cells and in more ventrally located epithelial cells during dorsal closure (Fig. 2, A and B) (*5*). Furthermore, the DFos mutant phenotype (Fig. 2, A through E) was enhanced by removal of one copy of *DJNK* (Fig. 2G) or *DJun* (Fig. 2F). *DFos* mutations also dominantly enhanced *DJNK* mutants (Fig. 2H). As in *DJun*, *DJNK*, and *DJNKK* mutant embryos, *dpp* expression in the leading edge but not in other tissues at this stage was abolished in *DFos* mutant embryos (Fig. 2, I and J). Therefore, DJun and DFos control, probably as heterodimers, *dpp* expression in the leading edge cells.

In vertebrates, c-Jun and c-Fos activities are regulated at various levels. Whereas c-Jun is widely expressed at low levels and activated primarily by NH_2-terminal phosphorylation by JNKs, c-*fos* expression is dynamic and activated in response to various extracellular stimuli (*1*). A similar dichotomy of *DJun* and *DFos* regulation occurs in *Drosophila*: DJun is widely expressed during embryogenesis and is phosphorylated by DJNK (*3–5*, *10*), whereas *DFos* expression is dynamic (Fig. 3, A through H) (*3*). There is strong expression of *DFos* in leading edge cells and cells of the lateral epithelium (Fig. 3, E and F).

Expression of DFos in the lateral epithelia is reduced in Tkv and Put mutant embryos but is still detectable in the leading edge (Fig. 3I) (*15*). Therefore, not only does DFos control expression of *dpp* in the leading edge, but in a reciprocal manner, *DFos* expression is dependent on Dpp function in cells of the lateral epithelium. Similarly in late embryos, *DFos* expression in the endoderm depends on *dpp* expression in the overlaying visceral mesoderm. In dpp^{S4} mutant embryos, where *dpp* is expressed in the ectoderm but not in the visceral mesoderm (*16*), *DFos* expression in the underlying endoderm is greatly reduced (Fig. 3J). Activation of the Dpp signaling pathway is indeed sufficient to activate *DFos* expression. Expression of an activated Dpp receptor, Tkv^{QD}, in 14 stripes in the ectoderm of developing em-

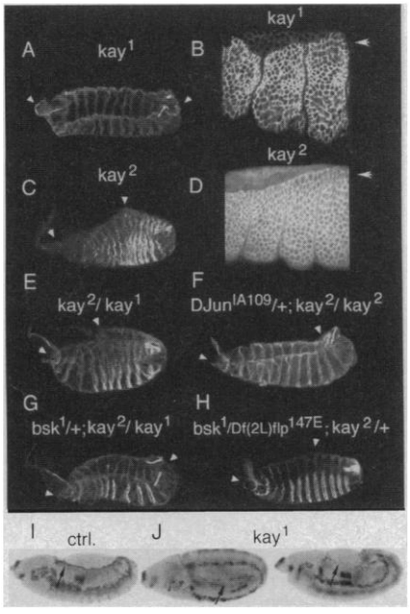

Fig. 2. DFos acts downstream of the DJNK pathway during dorsal closure. (**A**) A *kay*^{1} homozygous mutant embryo, and (**B**) an anti-Coracle antibody staining of a *kay*^{1} homozygote. The lateral epithelial cells fail to stretch; the leading edge cells are marked by an arrow. Coracle is a band 4.1 homolog and marks the cell membranes (*25*). The antibody staining were done as in (*5*). (**C**) *kay*^{2} homozygotes show partial dorsal closure; (**D**) the corresponding Coracle antibody staining shows partial stretching of leading edge cells (marked by an arrow). (**E**) *kay* heteroallelic mutant combination. (**F**) Mutations in DJun act as a dominant enhancer of a hypomorphic *kay* mutant. The embryo is completely open dorsally [compare with (C)] (*26*). (**G**) DJNK, *basket* (*bsk*), acts as a dominant enhancer of *kay*. The embryo is also completely open dorsally [compare with (E)]. (**H**) *kay* mutations dominantly enhance a *DJNK* (*bsk*) hypomorphic mutant. (**I** and **J**) *dpp* is expressed in the leading edge cells but is missing in *kay*^{1} mutants: (I) wild-type control embryo; (J) *kay*^{1} mutant embryos. The arrows point to the leading edge cells. The embryo in (I) is at stage 13; the middle one in (J), at stage 11; and the right one, at stage 12. Stages according to (*27*).

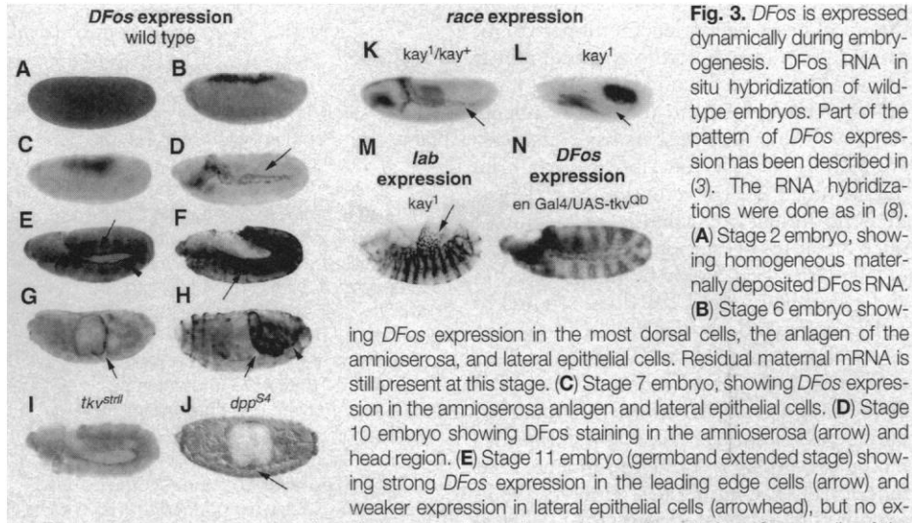

Fig. 3. *DFos* is expressed dynamically during embryogenesis. DFos RNA in situ hybridization of wild-type embryos. Part of the pattern of *DFos* expression has been described in (*3*). The RNA hybridizations were done as in (*8*). (**A**) Stage 2 embryo, showing homogeneous maternally deposited DFos RNA. (**B**) Stage 6 embryo showing *DFos* expression in the most dorsal cells, the anlagen of the amnioserosa, and lateral epithelial cells. Residual maternal mRNA is still present at this stage. (**C**) Stage 7 embryo, showing *DFos* expression in the amnioserosa anlagen and lateral epithelial cells. (**D**) Stage 10 embryo showing DFos staining in the amnioserosa (arrow) and head region. (**E**) Stage 11 embryo (germband extended stage) showing strong *DFos* expression in the leading edge cells (arrow) and weaker expression in lateral epithelial cells (arrowhead), but no expression in the amnioserosa, as well as the head region and muscle attachment sites. Some cells of the peripheral nervous system are also labeled. (**F**) Stage 12 embryo (germband retraction stage) showing prominent leading edge and strong lateral epithelial cells staining (arrow); rest of the pattern as in (E). DFos staining in lateral epithelial cells develops from stage 10 [compare (D) with (F)]. (**G**) Stage 15 embryo showing staining in a portion of the endoderm (arrow). (**H**) Stage 16/17 embryo, showing prominent perinuclear staining in the hindgut (arrow) and the Malpighian tubules (one of them is in the plane of focus, arrowhead). (**I**) *DFos* expression in lateral epithelial cells ventral to the leading edge cells is reduced in the *tkv*^{strII} mutant embryo. A stage 12 embryo [compare with (F)], showing staining only in the leading edge cells and very little, if any, in the lateral epithelial cells (*24*). Similar results were also obtained with another *dpp* receptor mutant, *put*^{135}. *tkv*^{strII} is a loss of function mutation in *tkv*, and *put*^{135} is an amorphic allele of *put* (*16*). (**J**) *DFos* expression is reduced in late embryos in the endoderm of *dpp*^{S4}mutants. Arrow points to residual expression; compare with (G). Mutant *dpp*^{s4} embryos lack *dpp* expression in the visceral mesoderm (*16*) and were recognized by the lack of the second midgut constriction. (**K**) *race* expression in the amnioserosa is missing in *kay* mutants. The embryo in (K) is heterozygous for the null *kay*^{1} mutation and shows *race* expression in the anterior and posterior midgut and in the cells of the amnioserosa (arrow). The homozygous *kay*^{1} mutant embryo in (**L**) is at a slightly later stage (note the position of the anterior and posterior gut endoderm, stained positive for *race* in both embryos). This embryo completely lacks expression in the amnioserosa cells (small arrow). This lack of amnioserosa *race* expression has also been documented for *dpp* mutant embryos (*18*, *19*). *DJun* and *bsk* mutant embryos, including embryos deprived of maternal and zygotic expression, show wild-type *race* expression (*21*). (**M**) *labial* expression in *kay* mutants is normal. The embryo is homozygous for *kay*^{1}; note cuticule formation in the ventral part of the embryo, as evidenced by nonspecific cuticular staining in a striped-like pattern (and its absence dorsally), and the graded nuclear Labial expression in the midgut (arrow). Antibody stainings were done with a Labial polyclonal antibody as in (*28*). (**N**) DFos is also downstream of the *dpp* pathway. The embryo shows strong ectopic DFos expression in stripes in the *engrailed* (*en*) expression domain. We expressed the activated Dpp receptor Tkv^{QD} in an *en* pattern by means of an *en Gal4* driver. The ectopic expression of DFos is superimposed on the normal DFos expression pattern [compare with (D)].

bryos with the use of an *engrailed* Gal4 driver (*16*) results in a corresponding pattern of *DFos* expression (Fig. 3N). During dorsal closure, *DFos* appears to be required in all epithelial cells, because restricted expression of *DFos* in the dorsal-most lateral ectoderm with a *pannier* GAL4 line (*17*) was not sufficient to rescue the dorsal-open phenotype of kay^1/kay^2 mutant embryos (Fig. 1F). Thus, DFos may be required in all ectodermal cells in order to activate target genes required for cell shape changes (Fig. 4).

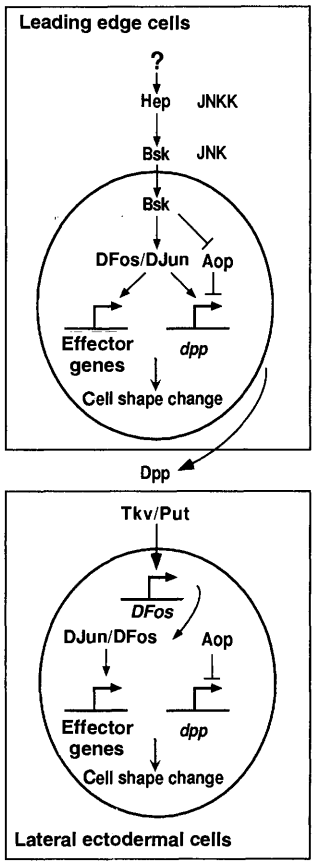

Fig. 4. Model of DFos function during dorsal closure. DFos is required both upstream and downstream of *dpp* during dorsal closure. Upon activation of the DJNK cascade in the leading edge cells by an unknown signal, activated DJNK translocates to the nucleus, where it phosphorylates the E26-specific (ETS) domain repressor Aop (the gene *aop*, or *anterior open*, is also known as *yan* and also acts in the *rl*/MAPK pathway) and DJun (*5*). Aop is inactivated by phosphorylation, whereas phosphorylation of DJun activates DJun. Both activated DJun and DFos are required for target gene expression. *dpp* is one of these target genes in the leading edge cells. Dpp then diffuses to ectodermal cells ventral to the leading edge cells, where it signals by means of its receptors Tkv and Put. This action then results in *DFos* transcription, upon which these lateral epithelial cells change shape. AP-1 activity is required for this last process, because DFos is also required in these cells for the change in cell shape. Thus, DFos is required in all lateral epithelial cells for stretching.

In the endoderm of late embryos, Dpp-induced expression of *DFos* correlates with induction of the homeotic gene *labial* (*lab*) in endodermal cells underlying *dpp*-expressing cells (*15*). Although ubiquitous expression of a dominant negative form of *DFos*, $DFos^{bZip}$, blocked *lab* expression in the endoderm (*15*), we observed normal levels of *lab* expression in *kay* mutants (Fig. 3L). This result indicates that in the endoderm DFos is not essential for Dpp-induced *lab* expression.

Independent of DJun, DFos also controls the expression of Dpp target genes during early embryonic development. Early *dpp* expression on the dorsal side of embryos induces expression of several genes, including *race*, which encodes a protein with homology to angiotensin-converting enzyme in the amnioserosa (*18*–*20*) (Fig. 3K). The *race* cis-acting sequences required for *dpp*-mediated expression contain AP-1 binding sites (*18*). Consistent with DFos-mediated direct activation of *race* through these AP-1 sites, *race* expression in the amnioserosa was abolished in *kay* mutant embryos (Fig. 3L). In contrast, *race* expression was normal in *DJun* or *bsk* mutant embryos (*21*). Thus, in addition to its role in controlling *dpp* expression in the leading edge, DFos also performs an essential function as mediator of Dpp during dorsal closure and during early embryogenesis, controlling Dpp target genes such as *race*. This early DJun-independent function of DFos may be mediated by DFos homodimers.

The joint requirement of DJun and DFos during dorsal closure provides the first genetic evidence for cooperation of these transcription factors during development. Defects in the dorsal joining of embryonic and adult epidermis observed in *DFos* and *hep* mutants suggest a common role of the DJNK pathway in joining of epithelial sheets. Control by AP-1 of epithelial cell morphology and possibly the composition of the extracellular matrix may be a universal phenomenon: During wound healing in vertebrates, a process that exhibits parallels with dorsal closure (*5*), TGF-β induces c-*fos* expression and AP-1 activity. The reciprocal regulatory relation between DFos and *dpp* in *Drosophila* appears to be conserved in mammalian cells. In mammalian myeloid cells, induction of c-*jun* and c-*fos* by serum or oncogenic v-*src* results in expression of TGF-β1 by direct activation of *TFG-β1* transcription by AP-1 (*22*). Furthermore, TGF-β induces AP-1 activity in keratinocytes during wound healing (*23*). The parallels between TGF-β and AP-1 signaling in mammalian cells and Dpp signaling and DFos and DJun signaling in *Drosophila* provide a striking example of evolutionary conservation of a complex regulatory pathway in epithelial cell morphogenesis.

REFERENCES AND NOTES

1. M. A. Cahill, R. Janknecht, A. Nordheim, *Curr. Biol.* **6**, 16 (1996); M. Karin, *Philos. Trans. R. Soc. London Ser. B* **351**, 127 (1996); ———, Z.-G. Liu, E. Zandi, *Curr. Opin. Cell Biol.* **9**, 240 (1997).
2. R. S. Johnson, B. M. Spiegelman, V. Papaioannou, *Cell* **71**, 577 (1992); R. S. Johnson, B. Lingen, V. E. Papaioannou, B. M. Spiegelman, *Genes Dev.* **7**, 1309 (1993); E. Hu *et al.*, *EMBO J.* **13**, 3094 (1994); Z.-Q. Wang *et al.*, *Nature* **360**, 741 (1992).
3. K. K. Perkins, G. M. Dailey, R. Tjian, *EMBO J.* **7**, 4265 (1988); K. K. Perkins, A. Admon, N. Patel, R. Tjian, *Genes Dev.* **4**, 822 (1990).
4. K. Zhang, J. R. Chaillet, L. A. Perkins, T. D. Halazonetis, N. Perrimon, *Proc. Natl. Acad. Sci. U.S.A.* **87**, 6281 (1990).
5. J. R. Riesgo-Escovar and E. Hafen, *Genes Dev.* **11**, 1717 (1997).
6. X. S. Hou, E. S. Goldstein, N. Perrimon, *ibid.*, p. 1728.
7. L. Kockel, J. Zeitlinger, L. M Straszewski, M. Mlodzik, D. Bohmann, *ibid.*, p. 1748.
8. J. R. Riesgo-Escovar, M. Jenni, A. Fritz, E. Hafen, *ibid.* **10**, 2759 (1996).
9. B. Glise, H. Bourbon, S. Noselli, *Cell* **83**, 451(1995).
10. H. K. Sluss, Z. Han, T. Barrett, R. J. Davis, Y. T. Ip, *Genes Dev.* **10**, 2745 (1996).
11. B. Glise and S. Noselli, *ibid.* **11**, 1738 (1997).
12. G. Jürgens, E. Weischaus, C. Nüsslein-Volhard, H. Kluding, *Roux's Arch. Dev. Biol.* **193**, 183 (1984); C. Nüsslein-Volhard, E. Wieschaus, H. Kluding, *ibid.*, p. 267.
13. Mutations of *kay* were mapped to the cytological position 99B10/C1 with *DF(3R)01215*: kay^1 fails to complement the deficiency and behaves genetically as a null allele, whereas kay^2 complements the deficiency. If, however, the cross is repeated in an $In(1)z^{ae(bx)}$ homozygous mutant background, which inhibits transvection, then a fraction of the $kay^2/DF(3R)01215$ embryos die with mild dorsal-closure phenotypes.
14. A. H. Brand and N. Perrimon, *Development* **118**, 401 (1993). We expressed the *DFos* cDNA in the embryonic ectoderm using the 69B Gal4 driver. We crossed UAS-*DFos* $kay^2/TM3$ to 69B $kay^1/TM3$ flies and scored the progeny; no embryos with a dorsal-open phenotype were found.
15. S. Eresh, J. Riese, D. B. Jackson, D. Bohmann, M. Bienz, *EMBO J.* **16**, 2014 (1997); M. Bienz, *Semin. Cell. Dev. Biol.* **7**, 113 (1996); J. Riese, G. Tremml, M. Bienz, *Development* **124**, 3353 (1997).
16. D. L. Lindsey and G. G. Zimm, *The Genetics and Biology of* Drosophila melanogaster (Academic Press, San Diego, CA, 1992).
17. P. Heitzler, M. Haenlin, P. Ramain, M. Calleja, P. Simpson, *Genetics* **143**, 1271 (1996).
18. J. Rusch and M. Levine, *Development* **124**, 303 (1997).
19. K. Tatei, H. Cai, Y. T. Ip, M. Levine, *Mech. Dev.* **51**, 157 (1995).
20. R. P. Ray, K. Arora, C. Nüsslein-Volhard, W. M. Gelbart, *Development* **113**, 35 (1991).
21. J. Riesgo-Escovar and E. Hafen, unpublished results.
22. S. J. Kim *et al.*, *Mol. Cell. Biol.* **10**, 1492 (1990); M. C. Birchenall-Roberts *et al.*, *ibid.*, p. 4978.
23. J. J. Woessner, *FASEB J.* **5**, 2145 (1991).
24. Of the 154 embryos examined from a tkv^{strII}/CyO stock hybridized with a *DFos* RNA probe, 36 had little or no staining in the lateral epithelial cells ventral to the leading edge cells, whereas 118 had a wild-type staining pattern. This distribution conforms statistically to a 1:3 ratio, as expected, because only one in every four embryos was a homozygous mutant for tkv^{strII}.
25. R. G. Fehon, I. A. Dawson, S. Artavanis-Tsakonas, *Development* **120**, 545 (1994).
26. Mutant embryonic cuticles were examined and

counted. Of the 98 cuticles examined for Fig. 2F, 44 were completely open dorsally (like the example in Fig. 2F), whereas 54 were only partially open dorsally (like Fig. 2C). This distribution corresponds statistically to a 1:1 ratio, consistent with half of the mutant *kay*^{2} embryos having received a mutant DJun allele and the other half having received a balancer chromosome, wild type for *DJun*. For Fig. 2G, 311 cuticles were examined; 151 were completely open dorsally (like Fig. 2G), and 160 were only partially dorsal open (like Fig. 2E). The distribution statistically conforms to a 1:1 ratio, as expected from half of the mutant embryos having received a mutant *bsk*^{1} allele, and half a balancer chromosome, wild type for *bsk*. All mutant *kay*^{2} or *kay*^{1}/*kay*^{2} cuticles examined were always only partially open dorsally. For Fig. 2H, 47 embryos were examined: 21 were three-quarters or more open dorsally (like Fig. 2H), and 26 were half or less open dorsally [see (*8*) for examples]. This distribution also corresponds statistically to a 1:1 ratio, as expected from half of the mutant *bsk*^{1}/*Df(2L)flp*^{147E} having received a mutant *kay*^{2} allele, and half a balancer chromosome. In all tests here and in (*24*), significance was assayed by a chi-squared test and was found in all cases to be $P < 0.05$.

27. J. Campos-Ortega and V. Hartenstein, *The Embryonic Development of* Drosophila melanogaster (Springer Verlag, New York, 1985).
28. D. Nellen, R. Burke, G. Struhl, K. Basler, *Cell* **85**, 357 (1996).
29. We thank K. Basler, B. Dickson, S. J. Leevers, and P. Mitchell for critical reading of the manuscript and especially K. Dücker for insightful discussions. J.R.R.-E. was a recipient of a Human Frontiers Science Program (HFSPO) postdoctoral fellowship, and E.H. is supported by grants from the Swiss National Science Foundation and the HFSPO.

14 July 1997; accepted 25 September 1997

Requirement for CD44 in Activated T Cell Extravasation into an Inflammatory Site

Heather C. DeGrendele, Pila Estess,* Mark H. Siegelman

Leukocytes extravasate from the blood into inflammatory sites through complementary ligand interactions between leukocytes and endothelial cells. Activation of T cells increases their binding to hyaluronate (HA) and enables CD44-mediated primary adhesion (rolling). This rolling could be induced in vivo in murine $V_\beta8^+$ T cells in response to specific superantigen stimulation; it was initially found in lymph nodes, then in peripheral blood, and finally within the peritoneum, the original inflamed site. The migration of $V_\beta8^+$ cells into the peritoneal cavity was dependent on CD44 and HA, as shown by inhibition studies. Thus, CD44-HA interactions can target lymphocytes to specific extralymphoid effector sites.

The compartmentalization, organization, and function of the immune system has engendered the development of specialized trafficking and recirculation patterns for subsets of lymphocytes that differ from those of other leukocytes. In particular, tissue-specific migration pathways of effector and memory lymphocyte subsets have been shown to be distinct and in part attributable to adhesion receptors they express (*1*–*4*). Since the inception of the model of sequential receptor engagement leading to leukocyte extravasation, only the selectin and integrin families of proteins have been implicated in primary (rolling) and secondary (firm) adhesion (*5*, *6*). The principal ligand for CD44, a marker of effector and memory lymphocytes, is HA (*7*), on which activated T cells can roll under physiologic shear stress conditions (*8*). In vivo activation of T cells and direct stimulation through the T cell receptor (TCR) results in CD44 capable of binding HA (*9*, *10*). Together, these findings suggest that CD44-HA interactions may be important for lymphocyte extravasation at inflammatory sites. We investigated whether T cell sensitization to antigen, occurring primarily within secondary lymphoid tissues, resulted in the induction of the "activated" HA-binding form of CD44 on antigen-specific cells; whether the stimulated cells bearing activated CD44 were mobilized into the peripheral circulation; and whether the activated CD44 on these cells then facilitated their extravasation into an inflammatory site.

Staphylococcal enterotoxin B (SEB) preferentially stimulates $V_\beta8^+$ T cells (*11*), which initially accumulate in the periphery and then are lost by 2 to 4 days after injection of SEB (*12*, *13*). We used intraperitoneal (ip) SEB injection of mice as an approach to obtain in vivo activated T cells, which we then examined by laminar flow and flow cytofluorometric analysis during the course of the response. For direct comparison of $V_\beta8$ composition and rolling activity, mesenteric lymph nodes (MLNs), peripheral blood, and peritoneal exudate leukocytes (PELs) were harvested at 4-hour intervals. The proportion of $V_\beta8^+$ cells in draining MLNs remained stable (at 15%) throughout this time course (Fig. 1A). Almost all $V_\beta8^+$ cells disappeared from peripheral blood by 4 hours after SEB injection, consistent with previous reports of sequestration of antigen-specific lymphocytes in secondary lymphoid organs at early time points after antigen injection (*14*–*16*). This drop was followed by a rapid rise of $V_\beta8^+$ T cells over the next 4 to 8 hours, followed by a gradual decline. In PELs, the percentage of $V_\beta8^+$ cells also initially decreased by 4 hours but then rose over the next 12 hours. The beginning of an accumulation of $V_\beta8^+$ cells in the peritoneal cavity was coincident with the peak of $V_\beta8^+$ cells in peripheral blood (Fig. 1A).

The HA-binding population in draining nodes after SEB injection was examined by flow cytometric analysis. After SEB treatment, 4% of all MLN lymphocytes bound fluoresceinated HA (Fl-HA), whereas binding was barely detectable in cells from control animals (Fig. 1B). This binding was inhibited by preincubation with monoclonal antibody (mAb) KM81, which inhibits the binding of activated CD44 to soluble HA (*17*). Of the total $V_\beta8^+$ lymph node population, 8.5% were $CD44^+$ and bound HA, whereas 17% of the $CD69^+$ and 28% of the lymphoblast populations were $CD44^+$ and bound HA. No HA binding was seen in $CD69^-$ cells, which suggested that CD44-dependent HA binding is a feature of activated but not resting cells. Thus, in vivo stimulation with SEB resulted in the activation of the specific $V_\beta8^+$ T cell subset within draining lymph nodes, which increased its HA binding and the potential for CD44-mediated primary adhesion.

The pattern of appearance of cells able to engage in CD44- and HA-dependent rolling interactions also showed sequential appearance in each anatomic compartment (Fig. 1C). MLN cells showed an early increase in rolling, which appeared 4 hours later in peripheral blood lymphocytes and not until 8 hours later in the peritoneal cavity. Although the timing of the appearance of rolling activity varied between experiments, the sequential appearance of both $V_\beta8$ cells and rolling activity in the three compartments in all experiments was maintained. Thus, the accumulation of rolling cells in peripheral blood and peritoneum paralleled the appearance of $V_\beta8^+$ lymphocytes in these sites, and it was consistent with the origination of CD44-mediated rolling cells within lymph nodes, with subsequent release into peripheral blood followed by extravasation into the inflamed peritoneum.

Cell populations were fractionated to identify which cells rolled after SEB injection (*18*). In all three compartments, the preponderance of the rolling activity was found in T cells, particularly the $V_\beta8^+$ sub-

Laboratory of Molecular Pathology, Department of Pathology, University of Texas Southwestern Medical Center, 5323 Harry Hines Boulevard, Dallas, TX 75235, USA.

*To whom correspondence should be addressed. E-mail: estess.pila@pathology.swmed.edu